JOURNAL OF SOLID STATE CHEMISTRY 58, 357–367 (1985)

Electron Microscopic Study of the System NiO–TiO_2

I. $Ni_{2(1+x)}Ti_{1-x}O_4$ Compounds

M. DE GRAEF,*,†,‡ P. A. SEINEN,* AND D. J. W. IJDO*

*Department of Inorganic Chemistry, Gorlaeus Lab., RU Leiden, The Netherlands; and †Department of Metallurgy and Materials Engineering, KU Leuven, Belgium

Received November 13, 1984

Transmission Electron Microscopy and High-Resolution Electron Microscopy were used to study $Ni_{2(1+x)}Ti_{1-x}O_4$ compounds. It is shown that the microstructure at high temperatures consists of NiO regions surrounded by thin lamellae of Ni_2TiO_4 spinel (space group *Fd3m*), analogous to the microstructure observed in the Fe_3O_4–Fe_2TiO_4 system. The pseudobinary phase diagram proposed in literature is shown to be incorrect. © 1985 Academic Press, Inc.

1. Introduction

The nonexistence of the pure spinel phase Ni_2TiO_4 has raised many questions during the last decade; X-ray powder diffraction data revealed that in part of the phase diagram of the NiO–TiO_2 system (i.e., for compositions between 63 and 97 mole% NiO) a nonstoichiometric spinel phase occurs at temperatures above 1380°C (Fig. 1). For a review of the literature on this system we refer to the papers by Armbruster *et al.* (*1–3*).

In (*3*) the spinel with composition $Ni_{2.44}Ti_{0.67}O_4$ was studied by means of single-crystal X-ray diffraction techniques; the structure was found to be that of a cation-excess spinel, i.e., there are more than 24 cations per unit cell. The normal spinel structure belongs to the space group *Fd3m* and consists of a cubic stacking of close-packed oxygen layers with cations in the octahedrally and tetrahedrally coordinated interstices. Assuming Ti^{4+} to be on the tetrahedral 8a positions, Ni^{2+} is found on the 16d sites and all oxygen atoms occupy the 32e positions (Fig. 2).

The extra Ni atoms in the $Ni_{2.44}Ti_{0.67}O_4$ compound were found on the second type of octahedral site 16c whereas only part of the 8a sites is randomly filled with Ti^{4+} cations. Structure refinements based on this model, using 51 independent reflections, resulted in a weighted *R*-factor of 0.033 (*3*). Chemical homogeneity was confirmed by electron microprobe measurements.

When this model was reinvestigated more closely some questions arose:

(1) Since the extra Ni atoms are found on the second type of octahedral site, some of these octahedra must share a face with the tetrahedra containing Ti; this face-sharing of coordination polyhedra, which is energetically unfavorable according to Pauling's third rule, should cause displacements of

‡ To whom correspondence should be addressed at Department of Metallurgy and Materials Engineering De Croylaan 2, B-3030 Heverlee (Leuven), Belgium.

0022-4596/85 $3.00

Copyright © 1985 by Academic Press, Inc.
All rights of reproduction in any form reserved.

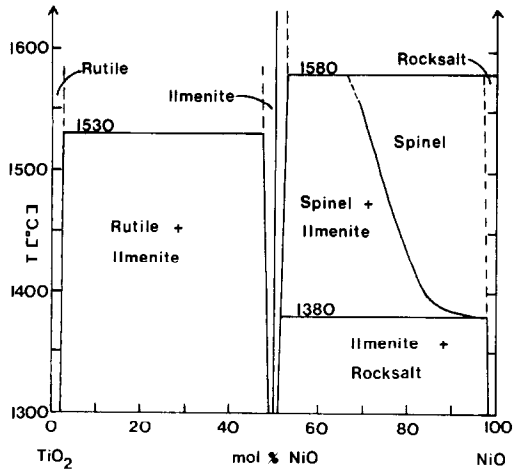

FIG. 1. High-temperature region of the binary phase diagram of the NiO–TiO_2 system (according to (*11*)).

the cations involved from their ideal positions. This is not observed experimentally (*3*).

(2) The experimentally observed fact that both Ni^{2+} and Ti^{4+} have a high octahedral site preference was used in literature to explain the nonexistence of the pure spinel phase Ni_2TiO_4 (Datta and Roy (*4*), Evans and Muan (*5*)); in other papers (Armbruster (*3*), Lager *et al.* (*6*)) Ti^{4+} is assumed to be on a tetrahedral site. If this assumption is correct, why then is it impossible to produce a pure Ni_2TiO_4 spinel?

(3) In literature several examples of nonstoichiometric phases, determined by X rays, can be found; more careful investigations sometimes revealed them to be mixtures of two different stoichiometric phases, frequently interwoven in a regular way (Bakker (*7*), De Graef *et al.* (*8*)). Therefore, we can ask the following question: was the structure determination in (*3*) performed on a real single crystal?

2. Specimen Preparation

Powders of $Ni_{2(1+x)}Ti_{1-x}O_4$ ($0.16 < x < 1$) were prepared from the pure oxides NiO and TiO_2. Samples containing between 70 and 95 mole% NiO were powdered and pressed into tablets. These were heated for 24 hr at 1000°C, crushed again, sealed into Pt tubes, and then heated for 60 hr at 1450°C. Subsequently all samples were quenched in water.

All samples were then investigated in a Philips X-ray powder diffractometer using Cu$K\alpha$ radiation (λ = 0.15418 nm).

Small amounts of powder were dispersed in alcohol and mounted on a 400-mesh copper grid coated with a Formvar/carbon holey film for investigation in an electron microscope. Electron diffraction patterns and bright field/dark field (BF/DF) image pairs were taken in a Siemens Elmiskop 102 equipped with a top-entry double tilting goniometer stage (±45 deg) operated at 100 kV. High-resolution experiments were performed on a JEM 200 CX, equipped with a top-entry high-resolution goniometer stage (±10 deg) operated at 200 kV; the spherical

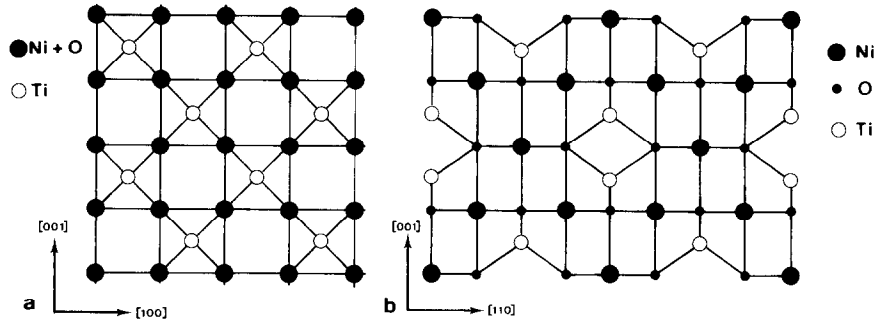

FIG. 2. [010] and [1$\bar{1}$0] projections of the perfect Ni_2TiO_4 spinel structure.

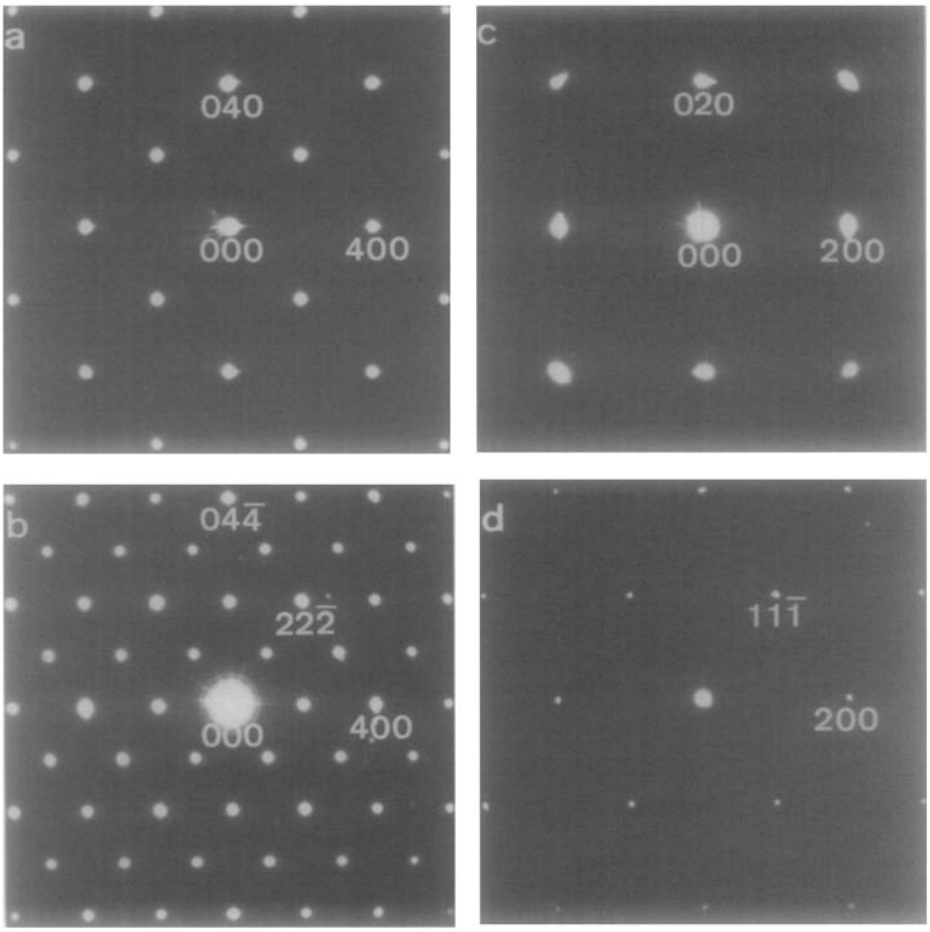

FIG. 3. Reciprocal lattice sections of a $Ni_{3.40}Ti_{0.30}O_4$ crystal fragment tilted along the [001] (a) and [011] (b) zone axis; (c) and (d) same sections for the pure NiO compound.

aberration constant for this instrument amounts to 1.2 mm. Image simulations for the high-resolution electron micrographs were carried out on the IBM Amdahl computer of the State University of Leiden using a batch version of the Real Space method developed by Van Dyck and Coene (*9, 10*).

3. Results

(*a*) *X-Ray Diffraction Results*

All samples showed NiO as well as spinel reflections (in fact, the NiO reflections can be considered as a subset of the spinel reflections); with increasing Ti content the spinel reflections became sharper.

From 20 mole% TiO_2 on, ilmenite reflections appeared, in agreement with the observations of Armbruster (*2*) and Laqua *et al.* (*11*). For the quenching temperature used in this work (1450°C) all X-ray observations seemed to be in complete accordance with the phase diagram of the NiO–TiO_2 system, as proposed by Laqua *et al.* (*11*).

(*b*) *Electron Microscopic Observations*

Selected-area electron diffraction patterns were obtained from all spinel samples

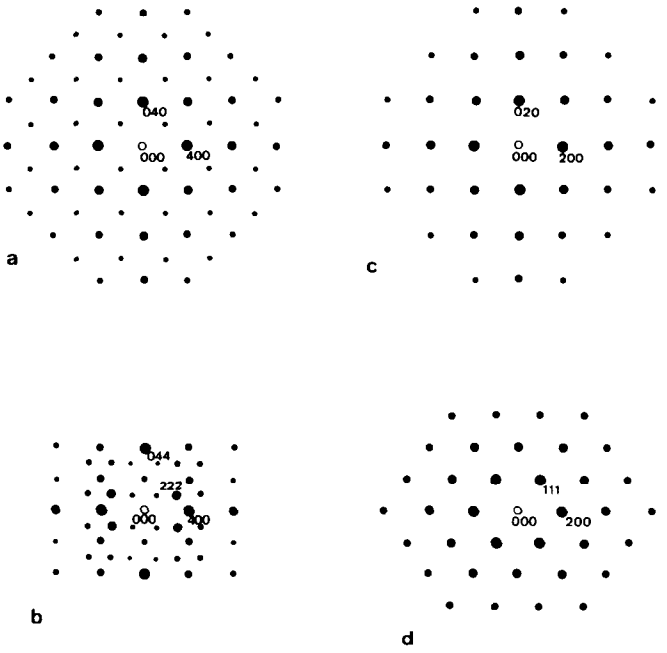

FIG. 4. Simulated electron diffraction patterns, using the kinematical diffraction theory, for the same sections as Fig. 3 (see text).

for several different orientations. The most prominent reciprocal lattice sections are shown in Fig. 3; all indices in (a) and (b) refer to the spinel reference system (a = 0.8348 nm). For comparison the same sections of the pure NiO compound (quenched from 1450°C) are also shown (c and d). Some reflections, such as the $(222)_{Sp}$-type reflections appear quite strong whereas they should be weak, according to the kinematical diffraction theory; the simulated diffraction patterns are shown in Fig. 4. There are two possible explanations for this effect: dynamical diffraction effects such as double diffraction can cause the reflection to become strong (this also explains the presence of the $(200)_{sp}$ reflection), or NiO domains are still present in the sample (the $(111)_{NiO}$ reflection is rather strong and coincides with the weak spinel reflection). Since reflections of the type $(110)_{NiO}$ = $(220)_{Sp}$ clearly are characteristic of the spinel structure and originate from regions which contain cations in tetrahedral positions (*12*) by taking a dark-field image using one of these reflections should reveal whether or not the crystal is chemically homogeneous. Figure 5 shows a BF/DF image pair obtained from a sample with composition $Ni_{3.40}Ti_{0.30}O_4$ oriented along the [001] direction; NiO domains surrounded by thin spinel lamellae are clearly present. Note that most of the spinel domains are more or less aligned along the cubic [100]-type directions.

The average domain size depends very sensitively on the amount of Ti^{4+} present, as shown in Fig. 6; the Ti content increases from (a) to (c) as indicated. Note the different scales. The domain shape also changes with increasing Ti content: from a fairly rectangular shape at low Ti content the NiO domains shrink to curved (sometimes elliptical) regions at high Ti content. This could indicate that part of the domain formation mechanism is dominated by a surface energy term.

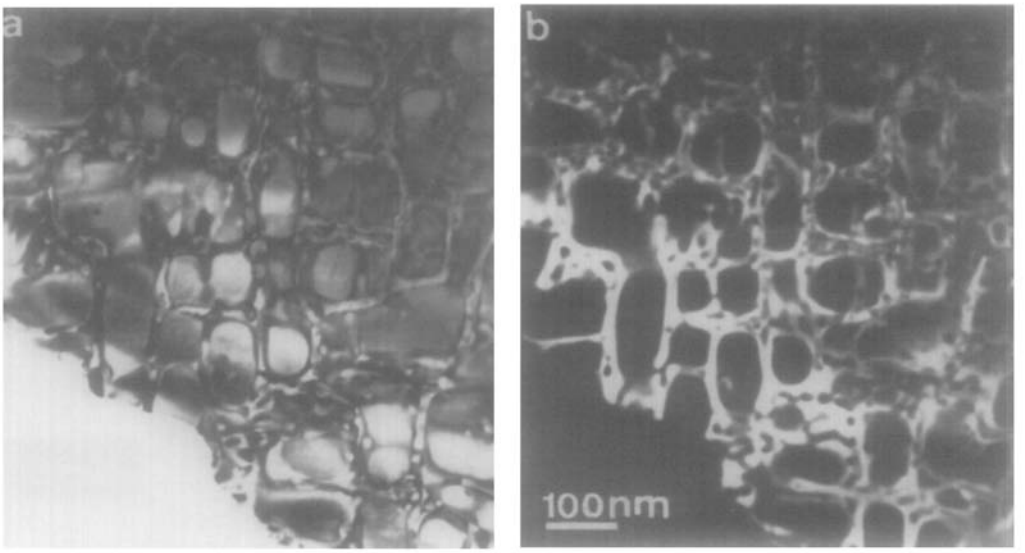

FIG. 5. Bright-field (a) and dark-field (b) electron micrographs of a crystal fragment of composition $Ni_{3.40}Ti_{0.30}O_4$ using the $(220)_{Spinel}$ reflection.

The largest NiO domains were found in a sample containing 5 mole% TiO_2 and had an average volume of approximately 10^7 nm^3, which is below the resolution limit of an electron microprobe instrument as illustrated in Fig. 7; here a comparison is made between a SEM picture of a representative spinel crystal (a) and a TEM picture of a small crystal fragment, close to the [100] orientation (b). Both samples have approximately the same composition.

In both pictures a terrace-like structure can be observed; as far as the distance between succeeding steps is concerned, Fig. 7b can be compared with the encircled region in Fig. 7a. Taking into account the fact that the common resolution limit of an electron microprobe instrument amounts to

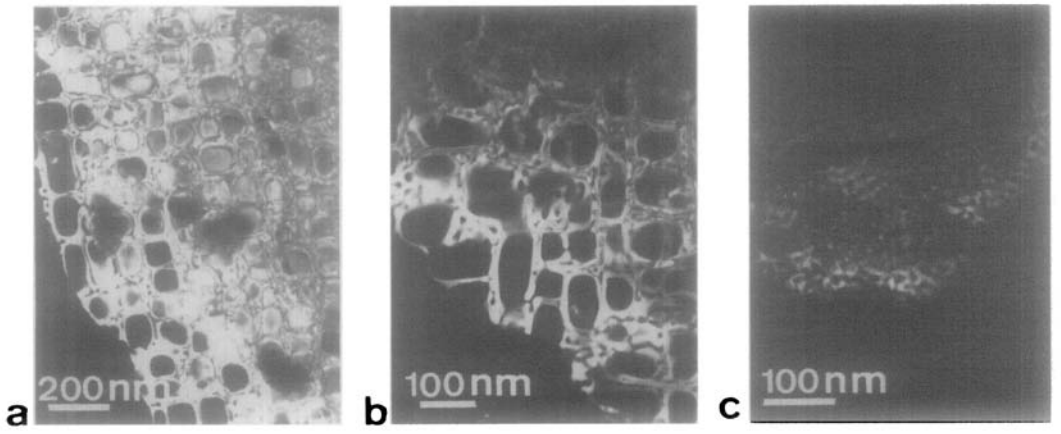

FIG. 6. Dark-field images of samples containing 5 (a), 10 (b), and 20 (c) mole% TiO_2. The size of the NiO domains decreases with increasing Ti content.

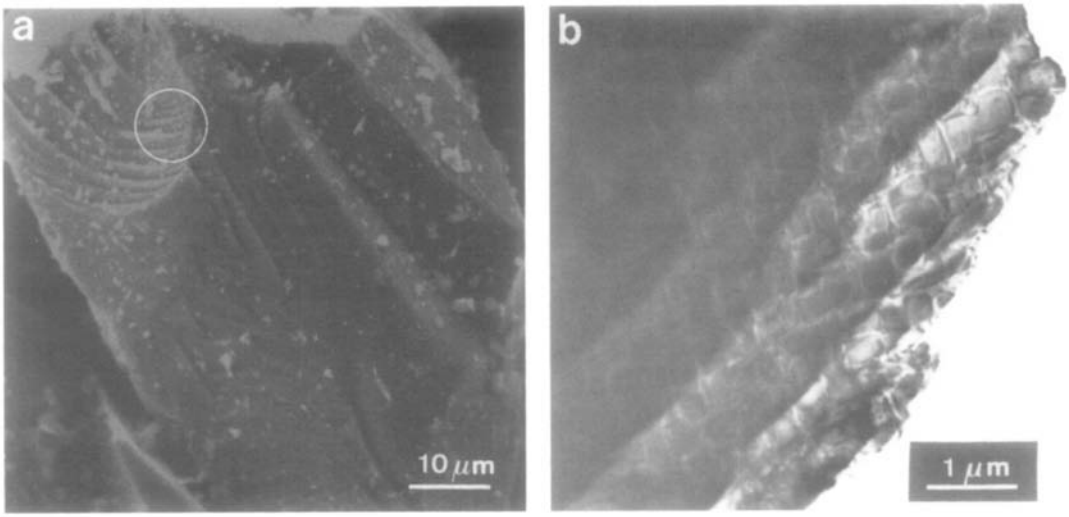

FIG. 7. (a) SEM picture of a representative spinel crystal, showing a terrace-like surface-structure. (b) TEM picture of a sample of approximately the same composition as (a) showing the relative size of the surface steps and the NiO domains.

about 10^9 nm^3, which is still two orders of magnitude larger than the maximum domain size observed by electron microscopy, it is obvious that the electron microprobe experiments carried out in (*1*) showed chemically homogeneous spinel crystals; domain formation of this size cannot be observed by scanning electron microscopy. Therefore all single-crystal structure determinations in (*3*) and (*5*) should be interpreted with great care in terms of the observed domain formation.

(*c*) *High-Resolution Electron Microscopy*

1. Observations. Looking at the projections of the spinel structure in Fig. 2 it is obvious that both viewing directions are very well suited for high-resolution observations; first of all, it should be noted that the spinel structure can be considered as a column structure when viewed along a [110]-type direction, i.e., only atoms of the same type superpose along this direction. Taking into account the point resolution of the electron microscope (which is about 0.26 nm for the JEM 200 CX) it should be possible to observe individual Ti and Ni columns. Furthermore, the [110] section contains information about the close-packed oxygen planes and therefore one should be able to observe any misfit between rock salt and spinel regions in this orientation.

In the [001] projection, on the other hand, the distance between different Ti columns is large enough to be resolved. Through-focus series were obtained for both beam directions. Figure 8 shows a high-resolution electron micrograph of a sample containing 10 mole% TiO_2, oriented along a [110]-type direction. Looking at this picture under a low angle reveals that there is no misfit at all between rock salt and spinel regions; all lattice planes cross the boundaries continuously. Optical diffraction patterns taken across the region indicated are shown in insets 1 (NiO) and 2 (Ni_2TiO_4).

In the area indicated by an arrow a rather smooth transition from rock salt to spinel structure can be observed whereas in other regions the boundary plane is confined to a

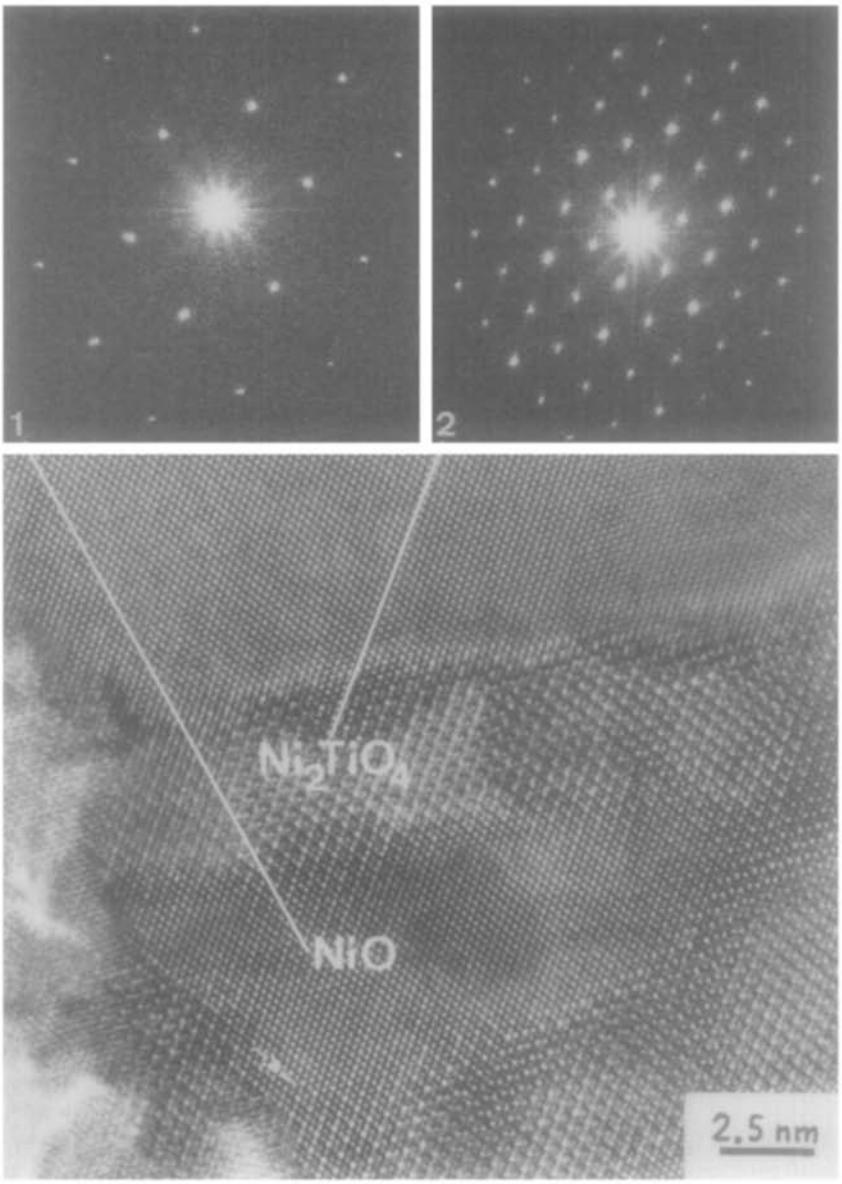

FIG. 8. High-resolution electron micrograph of a region oriented along a ⟨110⟩ type zone axis; insets (1) and (2) show optical diffraction patterns of NiO and Ni_2TiO_4, respectively. Note that lattice rows cross the domain boundaries continuously (without any misfit).

much smaller area. This can be interpreted in two ways: either the boundary plane is inclined to the electron beam, thereby giving rise to a broad region of overlap, or there is no real boundary present and both structures can change continuously from one into the other.

From our results, it seems that both interpretations are valid, depending on the Ti concentration: for low Ti content (i.e.,

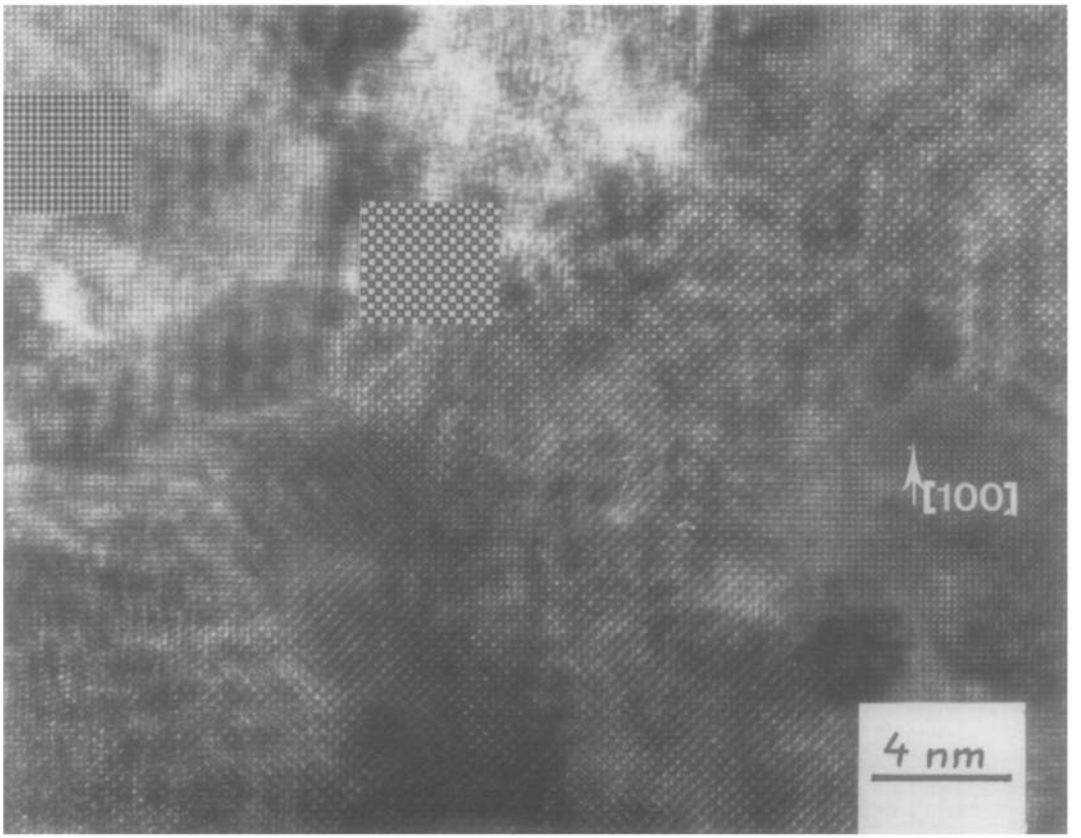

FIG. 9. High-resolution electron micrograph of a region oriented along a ⟨001⟩ direction (composition 20 mole% TiO_2); NiO and Ni_2TiO_4 regions are clearly visible. Insets show simulated images (see text).

large NiO domains) the domain walls are planar and well localized. With increasing Ti content (i.e., decreasing NiO-domain size) it becomes more difficult to define a boundary plane. For compositions close to the curved solid line in the phase diagram of Fig. 1 spinel and rock salt regions can no longer be completely separated, as illustrated in Fig. 9; here a region is shown of a sample with composition 20 mole% TiO_2 in a [001] orientation. The transition from rock salt to spinel is clearly spread out over several unit cells of NiO.

2. *Image simulations.* The Real Space method used for all image simulations in this work is an improved version of the more familiar multislice techniques (*13*); the propagation of electrons between subsequent slices is described in real space instead of reciprocal space, thereby decreasing the computation time. All simulations were performed for the perfect NiO and Ni_2TiO_4 structures and for perfectly axial illumination. Beams up to 0.7 nm^{-1} were included in the objective aperture.

Due to the fact that all samples appeared as nearly perfect NiO regions surrounded by very small fragments of spinel, it was very difficult to find Ni_2TiO_4 regions that were large enough to obtain a good match with the simulated images. Especially the [110] type of section proved to be rather difficult in this regard. The projected space group symmetry of the spinel structure

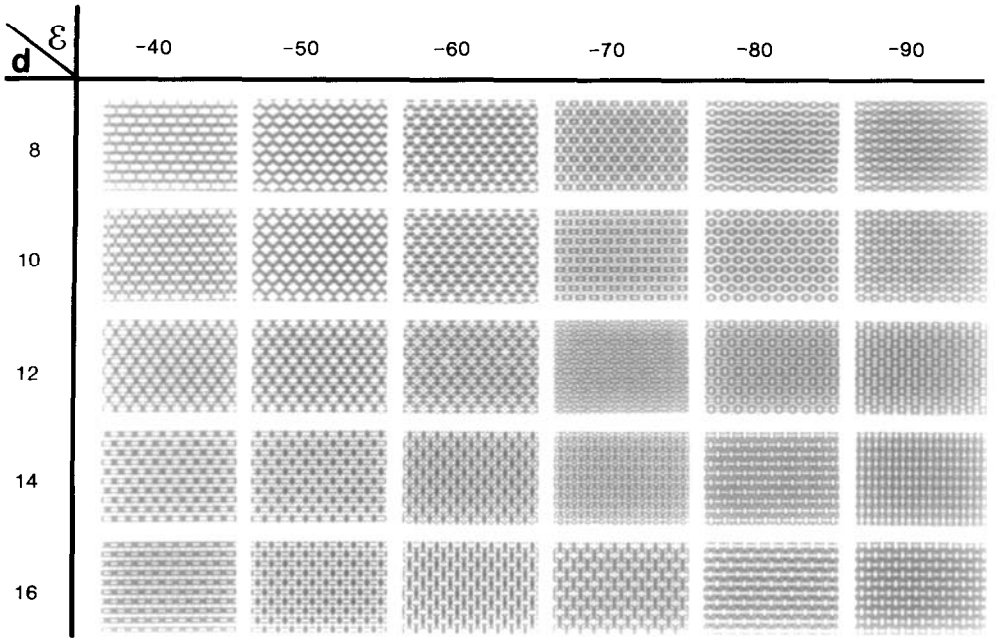

FIG. 10. Simulated images of ⟨110⟩-Ni_2TiO_4 using the Real Space method; image contrast varies very strongly with defocus ε and crystal thickness d.

model, however, fits very nicely with the observed symmetry for both ⟨110⟩ and ⟨001⟩ viewing directions.

Figure 10 shows a matrix of image simulations of Ni_2TiO_4 spinel in the [110] orientation for crystal thicknesses of 8 to 16 nm and microscope defocus values ranging from −40 to −90 nm. Clearly the image contrast is very sensitive to variations both in microscope defocus and crystal thickness. This is not the case, however, for the ⟨001⟩ orientation: image contrast in $\langle 001 \rangle_{NiO}$ proved to be very insensitive to both defocus and thickness. The inset on the left-hand side of Fig. 9 shows a simulation for a thickness of 14 nm and defocus value of −70 nm (close to the Scherzer defocus). Apart from a possible shift along a ⟨110⟩ type of direction, which cannot be measured experimentally, all images of NiO look exactly alike; therefore it was not possible to obtain information about defocus and crystal thickness from the NiO regions in Fig. 9.

Both insets serve as an example of the general image characteristics and should not be regarded as a quantitatively good match. To summarize our results, we can say that the symmetry of all high-resolution micrographs corresponds to that of the structure models; a detailed image simulation, however, was proved to be very difficult.

Discussion and Conclusion

The existence of microdomains, as reported in the previous sections, was already suggested by Laqua *et al.* (*11*); however, they did not perform any experiments with a resolution sufficient to observe them. For the same reason Armbruster and Lager could not have observed them either, their structure refinements are based on the

fact that a unit cell can be found which is repeated through the whole crystal volume. It is, however, inherent on the X-ray diffraction techniques that they give a statistical picture of the crystal, which is necessarily an average over several billions of unit cells. Structural features, such as large-scale intergrowth of different structural slabs (*7*) or domain formation cannot easily be recognized in this way. From our observations it follows that the structure determinations by Armbruster and Lager (*3*) are incorrect and have only a statistical value. It can in fact be shown that their results are compatible with our own observations: a weighted average of the NiO and Ni_2TiO_4 lattice occupation parameters (with weight factors proportional to the average domain sizes) results in a structure model which is comparable to the single-crystal model of (*3*), but this averaging is clearly not allowed.

The same type of domain formation was also observed in another system: electron microscopic investigations on natural crystals belonging to the system Fe_3O_4–Fe_2TiO_4 (Frost and Gai (*14*)) revealed that the mineral consisted of cubes of magnetite surrounded by thin lamellae of Ulvospinel. (Ulvospinel is an inverted spinel with Ti partially occupying the octahedral 16d sites whereas magnetite is an inverted spinel with respect to the ferrous and ferric cations).

The fact that (1) this type of domain formation occurs also in other (natural) systems (e.g., (*13, 17*)), and (2) that samples, used by Armbruster (*15*) for electron microprobe experiments, showed the same features as our own samples, when studied by transmission electron microscopy, leads to the conclusion that the assumed single-phase spinel region in the phase diagram of Fig. 1 is in fact a two-phase region. This conclusion has important consequences on the actual phase diagram: the two-phase "spinel" region is in contact with a two-phase "spinel–ilmenite" region. It is not yet clear whether or not the spinel in the "spinel–ilmenite" region is in itself a real "single-phase" spinel; preliminary experiments seem to indicate the coexistence of three different phases in this area: spinel, ilmenite, and rock salt. In order to get a clearer picture of the actual phases present in this system, a thorough investigation of the ternary Ni–Ti–O phase diagram will be performed, the results of which will be presented in a forthcoming paper (*16*).

From our results it is not possible to obtain detailed information about the actual lattice sites occupied by the Ti^{4+} cations; the high-resolution simulations based on the normal spinel structure model showed a good qualitative agreement with the experimental micrographs, but this does not prove that all Ti^{4+} is on tetrahedral sites, neither does it prove that there are no vacant oxygen polyhedra present. As far as the results from high-resolution electron microscopy are concerned the spinel regions are stoichiometric and nearly free of defects. Other techniques, such as EXAFS, could be useful to determine the coordination of the Ni^{2+} and Ti^{4+} cations.

The origin of the domain formation can perhaps be found by comparison with other systems, such as Fe_3O_4–Fe_2TiO_4, CoO–Co_2TiO_4, and Co_3O_4–Co_2TiO_4; the results of these investigations will also be presented in (*16*).

Two major conclusions can be drawn from the experimental results presented in this paper: the Ni-rich side of the NiO–TiO_2 phase diagram should be reconsidered as part of the ternary Ni–Ti–O phase diagram. The second conclusion is of a more general kind: whenever nonstoichiometry is involved (or suspected) X-ray diffraction techniques offer severe limitations as to the interpretation of the experimental results. Electron microscopy (or some other technique with the same spatial resolution) should be incorporated as a standard tool of

any structural investigation of nonstoichiometric compounds.

Acknowledgments

The authors would like to thank Dr. Th. Armbruster for providing us one of his samples, Dr. F. Mijlhoff for carrying out the image simulations, and Ir. O. Arkens for the SEM microprobe pictures.

References

1. TH. ARMBRUSTER, Ph.D. thesis, University of Bochum, Germany (1978).
2. TH. ARMBRUSTER, *J. Solid State Chem.* **36,** 275 (1981).
3. TH. ARMBRUSTER AND G. A. LAGER, *J. Phys. Chem. Solids* **42,** 725 (1981).
4. R. K. DATTA AND R. ROY, *Z. Kristallogr.* **121,** 410 (1965).
5. L. G. EVANS AND A. MUAN, *Thermochim. Acta* **2,** 277 (1971).
6. G. A. LAGER, TH. ARMBRUSTER, AND F. K. ROSS, *J. Appl. Crystallogr.* **14,** 261 (1981).
7. M. BAKKER, Ph. D. thesis, University of Leiden, The Netherlands (1982).
8. M. DE GRAEF, M. BAKKER, M. VAN HEMERT, J. VAN LANDUYT, AND S. AMELINCKX, *J. Solid State Chem.* **55,** 133 (1984).
9. D. VAN DYCK, *J. Microsc.* **119,** 141 (1980).
10. D. VAN DYCK AND W. COENE, *Ultramicroscopy* **15,** 29 (1984).
11. W. LAQUA, E. W. SCHULZ, AND B. REUTER, *Z. Anorg. Allg. Chem.* **433,** 167 (1977).
12. "International Tables for X-Ray Crystallography" (J. S. Kasper and K. Lonsdale, Eds.), Vol. I, Kynoch Press, Birmingham (1972).
13. A. J. SKARNULIS, S. IJIMA, AND J. M. COWLEY, *Acta Crystallogr. Sect. A* **32,** 799 (1976).
14. R. FROST AND P. L. GAI, *Acta Crystallogr. Sect. A* **36,** 678 (1980).
15. TH. ARMBRUSTER, private communication.
16. M. DE GRAEF AND D. J. W. IJDO, to be published.
17. M. BAKKER AND D. J. IJDO, to be published.